© The American Society of Gene & Cell Therapy

Adipose-derived Stem Cells as Therapeutic Delivery Vehicles of an Oncolytic Virus for Glioblastoma

Darnell T Josiah[1], Dongqin Zhu[1], Fernanda Dreher[1,2], John Olson[3], Grant McFadden[4] and Hannah Caldas[1,5,6]

[1]Brain Tumor Center of Excellence, Department of Neurosurgery, Wake Forest University School of Medicine, Winston-Salem, North Carolina, USA; [2]Department of Physiology, Faculdade de Medicina, Universidade Federal de Rio Grande do Sul, Porto Alegre, Brazil; [3]Center for Biomolecular Imaging, Wake Forest University School of Medicine, Winston-Salem, North Carolina, USA; [4]Department of Molecular Genetics and Microbiology, University of Florida, Gainesville, Florida, USA; [5]Section of Radiation Biology, Department of Radiation Oncology, Wake Forest University School of Medicine, Winston-Salem, North Carolina, USA; [6]Department of Cancer Biology, Wake Forest University School of Medicine, Winston-Salem, North Carolina, USA

Glioblastoma multiforme (GBM) accounts for the majority of primary malignant brain tumors and remains virtually incurable despite extensive surgical resection, radiotherapy, and chemotherapy. Treatment difficulty is due to its exceptional infiltrative nature and proclivity to integrate into normal brain tissue. Long-term survivors are rare, and median survival for patients is about 1 year. Use of adult stem cells as cellular delivery vehicles for anticancer agents is a novel attractive therapeutic strategy. We hypothesized that adipose-derived stem cells (ADSCs) possess the ability to home and deliver myxoma virus to glioma cells and experimental gliomas. We infected ADSCs with vMyxgfp and found them to be permissive for myxoma virus replication. ADSCs supported single and multiple rounds of replication leading to productive infection. Further, we observed no significant impact on ADSC viability. We cocultured fluorescently labeled GBM cells with myxoma virus–infected ADSCs in three-dimensional assay and observed successful cross infection and concomitant cell death almost exclusively in GBM cells. *In vivo* orthotopic studies injected with vMyxgfp-ADSCs intracranially away from the tumor demonstrated that myxoma virus was delivered by ADSCs resulting in significant survival increase. Our data suggest that ADSCs are promising new carriers of oncolytic viruses, specifically myxoma virus, to brain tumors.

Received 27 May 2009; accepted 19 October 2009; published online 10 November 2009. doi:10.1038/mt.2009.265

INTRODUCTION

Brain tumors account for 85–90% of all primary central nervous system tumors. It was estimated that 21,810 new cases of central nervous system tumors would be diagnosed in the United States in 2008 resulting in an estimated 13,070 deaths.[1–3] Anaplastic astrocytoma and glioblastoma multiforme (GBM) account for the majority of primary brain tumors. GBM remains virtually untreatable despite extensive surgical excision, radiotherapy, and chemotherapy. Treatment difficulty is due to their exceptional infiltrative nature and their proclivity to integrate extensively into normal brain tissue. Long-term survivors are rare, and median survival for patients with GBM is only about 12–16 months.[4,5] One experimental approach to treating malignant brain tumors involves the use of oncolytic viruses, and several have been tested experimentally and clinically.[6–8] The ideal oncolytic virus should have properties that include efficacy *in vitro* and *in vivo* against a broad range of tumors and relative selectivity for tumor cells so that normal, nontransformed cells are spared. Myxoma virus possesses these desirable characteristics and its tropism is highly restricted to European rabbits; additionally, there is a lack of acquired immunity to the virus in the human population.[9] Myxoma virus is a poxvirus and has a very large double-stranded DNA genome. It is a rabbit-specific virus that causes a lethal disease termed myxomatosis in the European rabbit (*Oryctolagus cuniculus*). Importantly, it is nonpathogenic for all other vertebrate species tested including humans.[10,11] Recent studies evaluated myxoma virus as a novel oncolytic agent against experimental gliomas *in vitro*, *in vivo*, and *ex vivo* against human malignant glioma surgical specimens.[12] It was shown that myxoma virus had oncolytic properties against human brain tumor cells both *in vitro* and *in vivo*.[12] However, myxoma virus was only effective when directly injected into the tumor bed.[12] This is a concern for highly infiltrative gliomas due to the poor biodistribution of myxoma virus as its oncolytic action will be restricted to the area of injection.

Experiments have shown that adult stem cells, such as neural, mesenchymal, and endothelial stem cells, have an uncanny ability to home to cancer cells and tumors, even moving through large areas of the body.[13–15] It has been demonstrated that neural stem cells, when implanted into experimental intracranial gliomas *in vivo* in adult rodents, distribute themselves quickly and extensively throughout the tumor bed.[16] When neural stem cells are implanted intracranially at distant sites from the tumor or implanted outside the central nervous system intravascularly, they migrate through normal tissue targeting the tumor cells.[16]

Correspondence: *Hannah Caldas, Brain Tumor Center of Excellence, Wake Forest University School of Medicine, 4th Floor NRC, Room 411, Medical Center Boulevard, Winston-Salem, North Carolina 27157, USA. E-mail: hcaldas@wfubmc.edu*

© The American Society of Gene & Cell Therapy

Similar results using human bone marrow–derived stem cells have shown that human bone marrow–derived stem cells also have a tropism for human gliomas after intravascular and local delivery.[17] Furthermore, it was shown that human bone marrow–derived stem cells can be used to deliver interferon-β to achieve tumoricidal effects.[17]

Some of the challenges in stem cell research are the expansion, propagation, and manipulation of functional adult stem cells. The clinical application of neural stem cells will be limited by logistic and ethical problems associated with their isolation and by potential immunologic incompatibility due to the requirement for allogeneic transplantation. Adult stem cells derived from mesodermal sources, such as bone marrow and adipose tissue, can be obtained from patients with greater ease and because autologous transplantation obviates immunologic incompatibilities. Adipose tissue is ubiquitous and uniquely expandable. Most patients possess excess fat that can be harvested making adipose tissue an ideal source for clinical research. Adipose-derived stem cells (ADSCs) have been examined as an alternative to bone marrow stromal cells and have been shown to be comparable.[18–20] Here, we evaluate the effects of myxoma virus infection produced and delivered by ADSCs as a novel therapeutic strategy for GBM. We show for the first time that ADSCs are permissive to and support a productive myxoma virus infection leading to successful cross infection of experimental GBM cells *in vitro* and *in vivo*. Moreover, myxoma virus–infected ADSCs administered intracerebrally in an orthotopic human malignant glioma model resulted in a significant increase of survival.

RESULTS

Myxoma virus productively infects ADSCs

We analyzed the permissiveness of ADSCs to vMyxgfp (green fluorescent protein expressing myxoma virus) by performing single-step and multistep viral growth curves. Single-step viral growth curves were performed at a high multiplicity of infection (MOI) to assess infectious progeny produced during a single replication cycle of myxoma virus. ADSCs were infected with vMyxgfp at an MOI of 10, and samples were harvested for infectious virus particles at 1, 4, 8, 12, and 24 hours after infection. All time point samples were titrated on BGMK cells via serial dilutions. Analysis of the single-step growth curves produced resembled a classical poxvirus replication curve reaching a nadir at ~4–8 hours after infection, which was then followed by a continuous increase to 24 hours after infection, at which point virus yield had reached maximum levels. Similar pattern of replication was observed in tumor cells, with the exception of a much rapid virus multiplication at the later time points (**Figure 1a**).

Multistep growth curves were performed at a lower MOI and for longer periods of time to quantify multiple rounds of viral replication and to assess cell-to-cell spread. ADSCs were infected with vMyxgfp at an MOI of 0.01, and samples were harvested for infectious virus particles at 12, 24, 72, and 96 hours after infection. All time point samples were titrated on BGMK cells via serial dilutions. Myxoma virus successfully underwent several rounds of replication and progressive cell-to-cell spread over time, as evident by the increasing virus titer, albeit at lower levels than in tumor cells (**Figure 1b**). Results of the single step and multistep growth curves demonstrate that ADSCs are permissive to and support both single and multiple rounds of myxoma virus replication.

Cytopathic effects of myxoma virus infection on ADSCs

We examined the effect of myxoma virus infection on cell viability of ADSCs and U-87 cells by using a cell viability assay. Cell viability was then measured at 48 hours after infection. We observed ~100% ADSC cell survival at 48 hours after infection, even at a high MOI of 100, compared to the uninfected ADSC control (MOI 0) (**Figure 2a**). However, U-87 cells were highly susceptible to the cytopathic effects of myxoma virus with approximately <40% cell survival at 48 hours after infection at MOIs of 10 and 100, compared to the uninfected U-87 cell control (MOI 0). Our results suggest that compared to myxoma virus infection of U-87 cells, the cytopathic effect was significantly less pronounced for ADSCs ($P = 0.03$; **Figure 2a**).

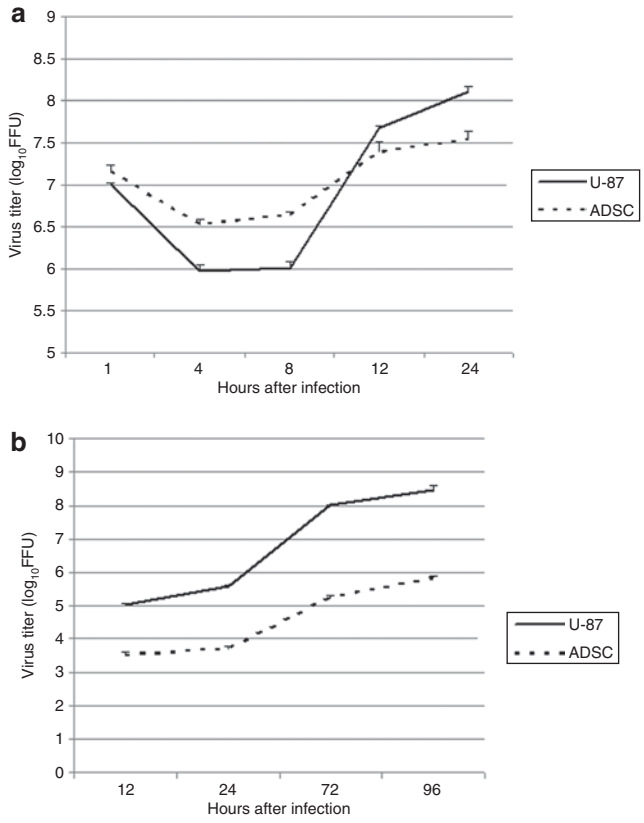

Figure 1 Myxoma virus productively infects adipose-derived stem cells (ADSCs). (**a**) Replication over the period of one replication cycle was investigated using high multiplicity of infection (MOI) single-step growth curves in ADSCs and U-87 cells. ADSCs and U-87 were infected with vMyxgfp (MOI = 10) followed by collection of cell lysates at the indicated times after infection. Viral titers were determined by titration on BGMK cells. Viral titer reached a minimum at 4–8 hours after infection, then continued to increase throughout the time period. (**b**) Replication over the period of multiple replication cycles was investigated using low MOI multistep growth curves in ADSCs. ADSCs and U-87 cells were infected with vMyxgfp (MOI = 0.01) followed by collection of cell lysates at the indicated times after infection. Viral titers were determined by titration on BGMK cells. Viral titer increased progressively indicating that myxoma virus successfully underwent multiple rounds of replication in ADSCs. FFU, fluorescent focus-forming unit.

© The American Society of Gene & Cell Therapy

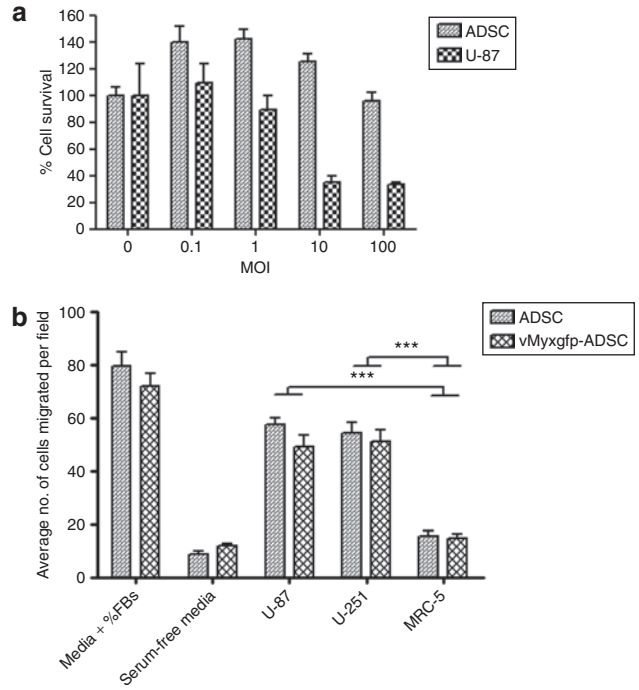

Figure 2 (a) Adipose-derived stem cell (ADSC) viability is not significantly affected by myxoma virus and is migratory toward U-87. Cytopathic effects of myxoma virus infection on ADSCs. ADSCs and U-87 cells were infected with different MOIs of vMyxgfp and evaluated by MTS assay at 48 hours after infection. U-87 cells were highly susceptible to myxoma virus killing, whereas ADSCs were significantly much less susceptible, maintaining high levels of cell viability. All conditions were done in triplicate and repeated in three separate experiments ($P = 0.0371$; error bars are SE). (**b**) Tropism of adipose-derived stem cells for human malignant glioma cells *in vitro*. ADSC migration in response to conditioned media from malignant glioma cell lines U-87 and U-251, and human fibroblasts (MRC-5). Whereas serum-free media and conditioned media from fibroblasts did not stimulate ADSC migration, conditioned media from U-87 and U-251 cells significantly stimulated ADSC migration through Matrigel ($P < 0.0001$). The migration capacity of ADSC was not affected by myxoma virus infection, MOI 10 ($P < 0.0001$). All conditions were done in triplicate; error bars are SE. FBS, fetal bovine serum; MOI, multiplicity of infection.

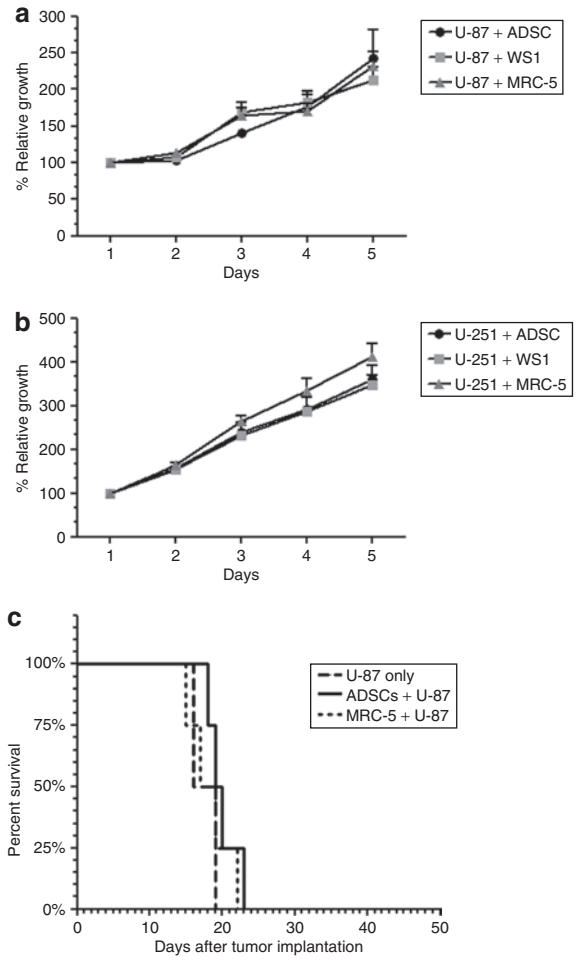

Figure 3 Adipose-derived stem cells (ADSCs) do not significantly impact the growth of human malignant glioma cells *in vitro* nor do they significantly affect animal survival. (**a**) The growth of U-87 cells were monitored by changes in red fluorescence levels in serum-free Matrigel for a period of 5 days in a bottom-read fluorescent plate reader. Stable red fluorescent U-87 malignant glioma cells were cocultured (10:1) with nonfluorescent ADSCs, nonfluorescent human skin fibroblasts (WS1), or nonfluorescent human lung fibroblasts (MRC-5) in a black-walled, clear bottomed 96-well plate. There was no significant difference in the growth rate of U-87 malignant glioma cells cultured in the presence of ADSCs compared with WS1 or MRC-5 ($P = 0.9950$). All conditions were done in triplicate and repeated in two separate experiments; error bars are SE. (**b**) Similar results were observed with U-251 cells. There was no significant difference in the growth rate of U-251 cells cultured in the presence of ADSCs compared with WS1 or MRC-5 ($P = 0.8934$). All conditions were done in triplicate and repeated in two separate experiments; error bars are SE. (**c**) The median survival for animals implanted with U-87 cells alone, with ADSCs, or with human lung fibroblasts (MRC-5) was 17.5, 19.5, and 18 days, respectively, $n = 4$ (log-rank, $P = 0.5088$).

Tropism of ADSCs for human malignant glioma cells *in vitro*

We hypothesized that the migratory capacity of ADSCs toward malignant gliomas is vital for their therapeutic potential, and factors released by malignant glioma cells may be potential mediators of the tropism of ADSCs for human malignant gliomas. To investigate ADSC tropism for malignant gliomas, we employed *in vitro* Matrigel migration assays using Transwell plates. We examined whether U-87 and U-251 cell lines were capable of stimulating migration of ADSCs. Accordingly, red fluorescently labeled ADSCs were placed in the upper wells on Matrigel and conditioned media from U-87 and U-251 cells, and MRC-5 fibroblasts grown in serum-free media were placed in the lower wells. A semiporous membrane (5 μm pores) separated the wells. Serum-free medium and medium supplemented with 10% fetal bovine serum were used as negative and positive controls, respectively. Migration was quantified by directly visualizing and counting the number of migrated ADSCs under fluorescence microscopy, in triplicate. In comparison, ADSCs exposed to serum-free media or to conditioned media from MRC-5 fibroblasts resulted in low levels of migrating ADSCs, whereas exposure to conditioned media from U-87 and U-251 cells produced significant ADSC migration ($P < 0.0001$) (**Figure 2b**). Migratory capacity of ADSC was not affected by infection with myxoma virus at an MOI of 10 ($P < 0.0001$; **Figure 2b**), suggesting that the migratory properties of ADSCs toward brain tumor cells remain unaltered upon myxoma virus infection.

© The American Society of Gene & Cell Therapy

ADSCs do not significantly impact the growth of human malignant glioma cells

To determine whether ADSCs affect the growth of glioma cells, we employed a three-dimensional tumor growth assay. It has been previously demonstrated that changes in relative red fluorescent intensity is proportional to changes in cell number, thus creating a relationship between cell growth and fluorescent intensity.[21] We cocultured U-87 and U-251 cells, stably transfected with the red fluorescent protein DsRed Express, at a 10:1 ratio with unlabeled ADSCs, unlabeled normal human skin fibroblast (WS1), or unlabeled normal human lung fibroblasts (MRC-5) in Matrigel and placed in a black-walled, clear bottomed 96-well plate. Quantification of malignant glioma cell fluorescence relative to day 1 for each experimental condition demonstrated no significant difference in growth rate of U-87 cells in the presence of ADSCs compared with the growth rate of U-87 cells in the presence of WS1 fibroblasts or MRC-5 fibroblasts ($P > 0.9$) (**Figure 3a**). Similarly, we did not observe a significant difference in the growth rate of U-251 cells in the presence of ADSCs compared with the growth rate of U-251 cells in the presence of WS1 fibroblasts or MRC-5 fibroblasts ($P > 0.8$) (**Figure 3b**). These results suggest that ADSCs do not significantly impact the growth of malignant glioma cells using this complex *in vitro* system.

To further elucidate the impact of ADSCs on malignant glioma tumor growth as a determinant of animal survival, we used an orthotopic brain tumor model. Human malignant glioma cell line U-87 was implanted in the right hemisphere of athymic nude mice using the stereotaxic system, as previously described.[22] We implanted U-87 cells alone, with ADSCs or normal human lung fibroblasts (MRC-5), and assessed for survival. The median survival for animals implanted with U-87 cells alone, U-87 cells coimplanted with ADSCs, and U-87 cells coimplanted with MRC-5 fibroblasts was 17.5, 19.5, and 18 days, respectively (log-rank, $P = 0.5$) (**Figure 3c**). This survival experiment suggests that ADSCs do not significantly impact animal survival in an orthotopic malignant brain tumor model.

In vitro oncolytic effect of ADSC produced myxoma virus on GBM cells

We examined the effect of myxoma virus produced by ADSCs on the growth of red fluorescent U-87 and U-251 cell lines *in vitro* by using a three-dimensional assay.[21] U-87 cells were cocultured with naive, uninfected ADSCs or vMyxgfp-infected ADSCs at a 1:1 ratio. We then analyzed cell populations by flow cytometry estimating the percentages of green fluorescent only cells (vMyxgfp-infected ADSCs), red fluorescent only cells (non-vMyxgfp-infected malignant glioma cells), red/green fluorescent cells (malignant glioma cells infected with myxoma virus produced in neighboring ADSCs), and negative, nonfluorescent cells (uninfected ADSCs). After 48 hours of coculturing, the percentage of red fluorescent cells (U-87 cells) were similar, ~40%, between the naive, uninfected ADSCs and vMyxgfp-infected ADSCs. However, after 96 hours of coculturing, there was a significant reduction in the percentage of red fluorescent only U-87 cells measured between the cocultured naive, uninfected ADSCs and the cocultured vMyxgfp-infected ADSCs, ~50 and 20%, respectively (**Figure 4a**).

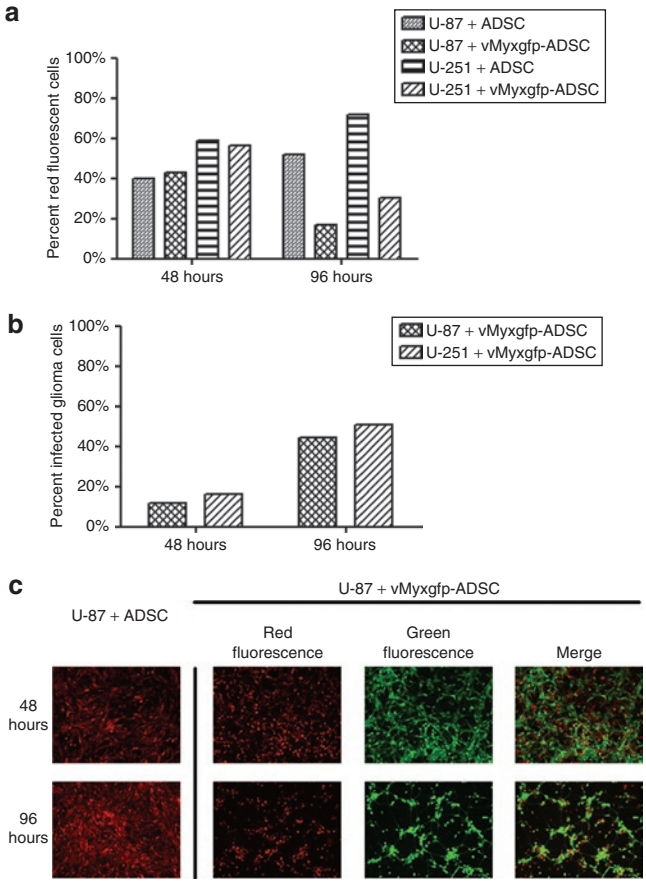

Figure 4 Adipose-derived stem cell–(ADSC) produced myxoma virus demonstrates oncolytic effect on human malignant glioma cells *in vitro*. (**a**) Stable red fluorescent U-87 or U-251 cells cocultured (1:1) with ADSCs or vMyxgfp-infected ADSCs, and analyzed by flow cytometry 48 hours after culturing. The percent of red fluorescent cells (U-87/U-251) was similar (~40%) between the cells cocultured with ADSCs and cells cocultured with vMyxgfp-infected ADSCs. In comparison, 96 hours after culturing, there was a significant reduction in the percent of red fluorescent cells (U-87/U-251) cocultured with vMyxgfp-infected ADSCs versus cells cocultured with ADSCs, ~20 and 50%, respectively. (**b**) Flow cytometry analysis of the percent of malignant glioma cells infected by myxoma virus produced by vMyxgfp-infected ADSCs at 48 and 96 hours after coculturing. The percent of infected glioma cells increased from ~15 to 45%, at 48 and 96 hours, respectively. Representative fluorescent images illustrating U-87. (**c**) Cells cocultured with ADSCs or vMyxgfp-infected ADSCs at a 1:1 ratio. Glioma cells are red fluorescent, and cells (ADSCs and glioma cells) infected with vMyxgfp are green fluorescent. Infected glioma cells are both red and green fluorescent.

To further investigate our hypothesis that vMyxgfp-infected ADSCs were producing myxoma virus leading to U-87 cell cross infection, we then analyzed the percentage of red/green fluorescent cells (malignant glioma cells infected with ADSC produced myxoma virus) by flow cytometry. After 48 hours of coculturing, the percentage of red/green fluorescent malignant glioma vMyxgfp-infected cells was ~15%. This percentage of red/green fluorescent malignant glioma vMyxgfp-infected cells increased to ~45% by 96 hours of coculture (**Figure 4b**) suggesting an increase of infected tumor cells over time. Similar results were observed using the U-251 cell line (**Figure 4a,b**).

© The American Society of Gene & Cell Therapy

At the 48- and 96-hour time point, representative fluorescent images were taken and visually corresponded to our observed flow cytometry data. The images in **Figure 4c** illustrate U-87 cells, indicated by red fluorescence, cocultured with naive, uninfected ADSCs or cocultured with vMyxgfp-infected ADSCs at a 1:1 ratio. Cells infected with vMyxgfp are green fluorescent, cells that are red fluorescent only are U-87 cells, and U-87 cells infected with vMyxgfp are both red and green fluorescent. These results offer proof of successful cross-infection of malignant glioma cells by ADSC produced myxoma virus. Additionally, U-87 cells infected with vMyxgfp produced by ADSCs displayed pyknotic morphology suggestive of cell death. Similar results were observed with U-251 cells (**Supplementary Figure S1**).

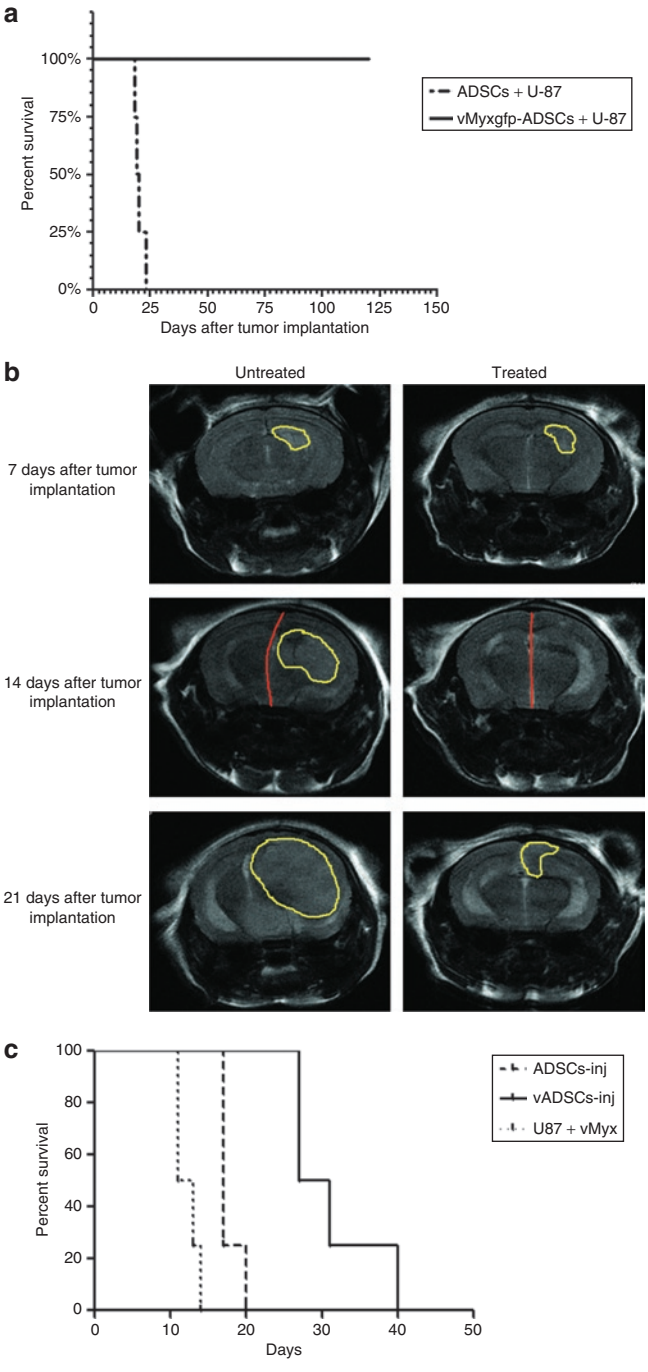

In vivo oncolytic effect of ADSC produced myxoma virus in an orthotopic malignant brain tumor model

As a proof of principle, we coimplanted U-87 cells with ADSCs or vMyxgfp-infected ADSCs at 1:1 ratios in the right hemisphere of athymic nude mice using the stereotaxic system, as previously described[22] and the animals followed for survival analysis until an experimental end point. The median survival for animals coimplanted with U-87 cells and ADSCs was 19.5 days (**Figure 5a**). The median survival for animals coimplanted with U-87 cells and vMyxgfp-infected ADSCs was not reached because none of the animals reached any of the predetermined experimental end points, and the experiment was arbitrarily terminated at 120 days (log-rank, $P = 0.0067$) (**Figure 5a**). This survival experiment suggests that vMyxgfp-infected ADSCs produced myxoma virus that successfully cross infected U-87 malignant glioma cells, and myxoma virus retained its oncolytic properties in an orthotopic malignant brain tumor model.

Therapeutic efficacy of ADSC produced myxoma virus on human malignant gliomas

We investigated the efficacy of ADSC to deliver myxoma virus on prolonging animal survival utilizing an established orthotopic malignant brain tumor model. Accordingly, we implanted U-87 cells into the right hemisphere of athymic nude mice, and 7 days later, when tumors had formed, we divided the animals into two groups; we administered a single intracranial, nonintratumoral injection of ADSCs or vMyxgfp-infected ADSCs into the right hemisphere ~1 mm anterior to the implanted tumor, and the animals were followed for survival analysis. Representative ADSC (control) and vMyxgfp-infected ADSC (treatment) animals were subjected to microMRI every 7 days, after U-87 cell implantation, for a period of 3 weeks to evaluate tumor size and visualize evidentiary anatomical perturbations. T2-weighted magnetic resonance imaging (MRI), 7 days after tumor implantation and prior to administration of ADSCs (controls) or vMyxgfp-infected ADSCs (treatment), demonstrated established brain tumors of comparable size in both the control and the treatment representative animals (**Figure 5b**). T2-weighted MRI, 14 days after tumor implantation and 7 days after a single intracranial, nonintratumoral injection of

Figure 5 Adipose-derived stem cell (ADSC)–produced myxoma virus has oncolytic effect on human malignant glioma cells *in vivo*. (**a**) U-87 cells were coimplanted with ADSCs or vMyxgfp-infected ADSCs (1:1) into the right hemisphere of athymic nude mice. Median survival was significantly longer in vMyxgfp-infected ADSC coimplanted animals compared with the ADSC coimplanted controls (median survival not reached for vMyxgfp-ADSCs versus 19.5 days; log-rank, $P = 0.0067$, $n = 4$). #Survival experiment arbitrarily terminated at 120 days. (**b**) T2-weighted magnetic resonance (MR) images 7 days after tumor implantation of untreated and treated representative animals before administration of a single intracranial, nonintratumoral injection of ADSCs (untreated) or vMyxgfp-ADSCs (treated). MR images show brain tumors of comparable size in both animals. Fourteen days after tumor implantation and 7 days after treatment, the untreated animal demonstrates midline shift and a larger brain tumor mass. The treated animal demonstrates a lack of midline shift, and no MR evidence of a brain tumor. Twenty-one days after tumor implantation and 14 days after treatment, the untreated animal demonstrates a significantly larger brain tumor mass than the treated animal that demonstrates a smaller recurrent brain tumor mass. (**c**) Treated animals survived significantly longer than ADSC-treated controls, 29 and 17 days, respectively (log-rank, $P = 0.0058$, $n = 4$).

© The American Society of Gene & Cell Therapy

ADSCs or vMyxgfp-infected ADSCs into the right hemisphere, demonstrated a progressively larger brain tumor and midline shift (attributable to mass effect caused by the growing tumor) in the control animal (**Figure 5b**). However, the vMyxgfp-infected ADSC-treated animal demonstrated a lack of midline shift, and no MRI evidence of a brain tumor (**Figure 5b**). T2-weighted MRI, 21 days after tumor implantation and 14 days after a single intracranial, nonintratumoral injection of ADSCs or vMyxgfp-infected ADSCs into the right hemisphere, further demonstrated a significantly larger brain tumor and increased midline shift in the control animal (**Figure 5b**). In comparison, the vMyxgfp-infected ADSC-treated animal demonstrated evidence of a smaller brain tumor (**Figure 5b**). This is also evident upon 3D reconstruction of all MRI slices and demonstrated in **Supplementary Videos S1 and S2**, and **Supplementary Materials and Methods**. The median survival for the ADSC control animals was 17 days compared to the vMyxgfp-infected ADSC treated animal median survival of 29 days. This survival experiment suggests that vMyxgfp-infected ADSCs delivered myxoma virus to malignant glioma *in situ* resulting in a significant decrease in tumor growth and size with a concomitant increase in animal survival (log-rank, $P = 0.0058$; **Figure 5c**).

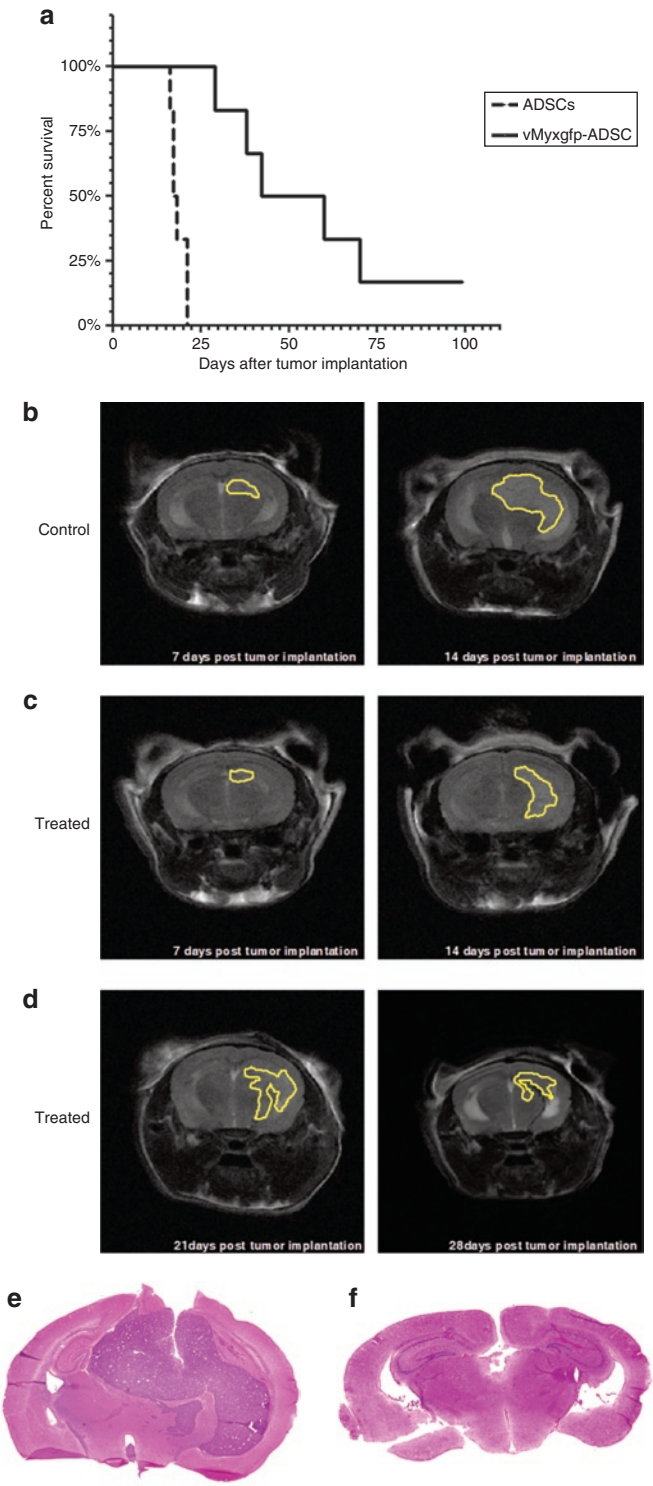

Multiple administrations of ADSC infected with myxoma virus produces long-term survival in an orthotopic human malignant brain tumor model

Based on the above studies, we hypothesized that repeated intracranial, nonintratumoral injections of vMyxgfp-infected ADSCs would enhance the therapeutic efficacy and produce longer animal survival and disease-free progressions. We implanted U-87 cells into the right hemisphere of athymic nude mice, and 7 days later when tumors had formed, we divided the animals into two groups; ADSC controls and vMyxgfp-infected ADSC treatment animals. We administered an intracranial, nonintratumoral (adjacent to the tumor site) injection of ADSCs or vMyxgfp-infected ADSCs into the right hemisphere ~1 mm anterior to the implanted U-87 cells, as previously described above. Fourteen days after tumor implantation and seven days after the first anteriorly placed intracranial, nonintratumoral injection of ADSCs or vMyxgfp-infected ADSCs into the right hemisphere, we administered another intracranial, nonintratumoral injection of ADSCs or vMyxgfp-infected ADSCs into the right hemisphere; however, this was placed ~1 mm posterior to the implanted U-87 cells. We alternated the placement (1 mm anterior or 1 mm posterior to the implanted U-87 cells) of four subsequent intracranial, nonintratumoral injection of ADSCs or vMyxgfp-infected ADSCs into the right hemisphere every 7 days for a total of six intracranial, nonintratumoral therapeutic administrations, and measured tumor progression and survival. The median survival for the ADSC control animals was 17.5 days compared to the vMyxgfp-infected ADSC treated animal median survival of 56.5 days (**Figure 6a**). This survival experiment suggests that multiple administrations

Figure 6 Multiple administrations of adipose-derived stem cells (ADSCs) infected with myxoma virus produces long-term survival in an orthotopic human malignant brain tumor model. (**a**) Animals with an established brain tumor treated with a multiple, temporally spaced, intracranial, nonintratumoral injection of vMyxgfp-ADSCs survived significantly longer than ADSC-treated controls, 56.5 and 17.5 days, respectively (log-rank, $P = 0.0007$, $n = 6$). (**b**) T2-weighted magnetic resonance (MR) images 7 days after tumor implantation and 7 days after administration of a nonintratumoral injection of ADSCs. (**c**) T2-weighted MR images 7 days after tumor implantation and 7 days after an administration of an intracranial, nonintratumoral injection of vMyxgfp-ADSCs anterior to tumor mass. (**d**) T2-weighted MR images 21 and 28 days after tumor implantation after weekly administration of intracranial, nonintratumoral injection of vMyxgfp-ADSCs. Tumors are delineated in yellow. Hematoxylin and eosin staining of representative (**e**) control and (**f**) treated tumors.

© The American Society of Gene & Cell Therapy

of vMyxgfp-infected ADSCs produce long-term survival in an animal model of human malignant glioma (log-rank, $P = 0.0007$; **Figure 6a**). Additionally, we observed disease-free progression in 20% of animals suggesting that multiple injections of vMyxgfp-infected ADSCs are an effective means at containing tumor growth. Representative ADSC (control) and vMyxgfp-infected ADSC (treatment) animals were subjected to microMRI every 7 days, after U-87 cell implantation, for a period of 4 weeks to evaluate tumor size and visualize evidentiary anatomical perturbations. T2-weighted MRI, 7 days after tumor implantation and prior to administration of ADSCs (controls) or vMyxgfp-infected ADSCs (treatment), demonstrated established brain tumors of comparable size in both the control and the treatment representative animals (**Figure 6b,c**). T2-weighted MRI, 14 days after tumor implantation and 7 days after a single intracranial, noninatratumoral injection of ADSCs or vMyxgfp-infected ADSCs into the right hemisphere, demonstrated a progressively larger brain tumor and midline shift (attributable to mass effect caused by the growing tumor) in the control animal (**Figure 6b**). The tumors in the control group became large and caused locomotory problems as well as neurologic defects resulting in the euthanization of the animals. However, the vMyxgfp-infected ADSC-treated animals demonstrated a lack of midline shift with a smaller tumor that remained contained over time (**Figure 6c,d**). Some of the treated animals were tumor-free by the end of the experimental period (100 days) (**Supplementary Figure S2**). We further analyzed the brains of control and treated animals to assess tumor size after euthanasia. Representative image of control treated animals shown in **Figure 6e** demonstrated a large tumor that invaded the contralateral side of tumor injection resulting in midline shift. The tumors presented higher degree of cellularity and increased number of mitotic figures. In contrast, representative images of treated animals showed very small tumors, with low degree of cellularity (**Figure 6e**).

DISCUSSION

This is the first demonstration of the potential applicability of ADSCs to deliver myxoma virus in an experimental model of GBM. It has been shown that myxoma virus has the ability to infect and kill human GBM cells *in vitro* and *in vivo*.[12,23] However, due to myxoma virus narrow host range and its lack of ability to productively infect normal nonleporine cells, such as untransformed brain cells, its efficacy was limited to the area of direct intratumoral injection without the capacity to infect and kill distant brain tumors.[12] Here, we report several important observations. First, we show that ADSCs are permissive to myxoma virus and are able to support a productive infection. This is a crucial aspect as myxoma virus replication must be at levels capable of causing successful cross infection of surrounded tumor cells. ADSCs have the ability to support multiple rounds of myxoma virus replication, allowing long-term viral replication, potentially maximizing the amount of time and virus available for delivery into brain tumors. Second, we observed ADSCs' ability to migrate to tumor cells, similar to other adult stem cells previously reported.[17,24]

We show that ADSCs infected with myxoma virus are able to successfully cross infect and kill GBM cells when cocultured *in vitro*; moreover, we show that ADSCs infected with myxoma virus produce a significant increase in survival in *in vivo* models of human malignant glioma. The potential ability of ADSCs to seek out all brain tumor cells and deliver oncolytic myxoma virus is of great therapeutic value given the invasive nature of GBM. Taken together, ADSCs can potentially act as "Trojan horses" that are capable of migrating and engrafting into GBM tumors and delivering myxoma virus to these tumor areas.

An important consideration for the clinical use of adult stem cells as therapeutic vehicles is the question of their augmentation on tumor size and growth. We found that uninfected, naive ADSCs do not significantly impact the growth of glioma tumor cells in the three-dimensional tumor growth *in vitro* model; further, they did not significantly impact the median survival of orthotopic glioma mouse models. This is in contrast to the study reporting enhancement of estrogen receptor positive breast cancer cells by human bone marrow stromal cells.[21] It is of great importance that ADSCs do not enhance brain tumor growth due to the confined space of the cranial vault where an enlarging mass could result in hastening neurologic dysfunction and worsening of symptoms.

The mechanism whereby ADSCs are permissive to myxoma virus remains to be elucidated. The permissiveness of human tumor cells has been reportedly linked to endogenously high levels of Akt;[25] whether this is also a factor for ADSCs remains to be determined. Myxoma virus narrow host range in nature, its potent oncolytic ability and the important fact that there has never been a report of myxoma virus infections in humans,[10–12] is a very attractive aspect in comparison to other therapeutic oncolytic viruses.[6–8,26] In this study, we show that there was a significant increase in animal survival when human glioma U-87 cells were co-injected with myxoma virus–infected ADSCs, and survival was also significantly increased in animals bearing U-87 orthotopic xenografts that received a single intracranial injection of myxoma virus–infected ADSCs.

Our studies form the proof of principle that a cellular carrier like ADSC is effective at delivering myxoma virus at sites distant from the injection site. This is an important consideration for translation due to the highly infiltrative nature of brain tumors. Future studies will investigate alternative delivery routes, such as intravascularly, and we hope to elucidate the mechanism of permissiveness of ADSCs to myxoma virus and the factors responsible for the migration of ADSCs toward brain tumor cells.

MATERIALS AND METHODS

Cell lines. GBM cell lines U-87 and U-251, and normal human skin and lung fibroblast (WS1 and MRC-5, respectively) cells were obtained from the American Type Culture Collection (Manassas, VA). ADSCs isolated via lipo-aspiration from healthy female donors were obtained from ZenBio (Research Triangle Park, NC). U-87, U-251, WS1, and MRC-5 cells were maintained in Dulbecco's modified Eagle's medium containing 10% fetal bovine serum and penicillin–streptomycin at 37 °C in a humidified atmosphere containing 5% CO_2. ADSCs were maintained in α-MEM supplemented with 10% defined fetal bovine serum (HyClone, Logan, UT) at 37 °C in a humidified atmosphere containing 5% CO_2 and used before passage 10.

U-87 and U-251 cell lines stably expressing the red fluorescent protein DsRed Express were generated by transfecting pDsRed Express C1 (Clontech, Mountain View, CA), and selection was performed with G418 (400 μg/ml) for 2 weeks. The cells were then subjected to fluorescence-activated cell sorting to isolate the highest expressers of DsRed Express,

© The American Society of Gene & Cell Therapy

over three sequential sort rounds. The resulting cell lines were tested for long-term expression of DsRed Express in the absence of G418, as well as phenotypic changes.

Virus. A derivative of myxoma virus (strain Lausanne), designated vMyxgfp, was kindly provided by G.M., University of Florida, Gainesville, FL. This virus contains a green fluorescent protein insert located between open reading frames M135R and M136R of the myxoma genome.[12]

Viral replication assays

Single-step growth analysis: ADSCs were infected with an MOI of 10 of vMyxgfp. The inoculum was allowed to adsorb for 1 hour, the virus was removed, and the wells were washed with 1× phosphate-buffered saline (PBS). Supplemented α-MEM was added to the wells, which were then incubated at 37 °C. ADSCs were collected via trypsinization at the indicated time points: 1, 4, 8, 12, and 24 hours after infection. After spinning for 5 minutes, the ADSCs were resuspended in 200 µl of hypotonic swelling buffer. The virus was released from infected ADSCs by three freeze–thaw cycles. Viral titers within the collected cell lysates were performed in BGMK cells. Briefly, BGMK cells were incubated with serial diluted lysates at 37 °C for 1 hour, washed with 1× PBS. Supplemented Dulbecco's modified Eagle's medium was added to the wells, and BGMK cells were incubated at 37 °C for 48 hours.

Multistep growth analysis: ADSCs were infected at an MOI of 0.01 of vMyxgfp. The inoculum was allowed to adsorb for 1 hour, the virus was removed, and the wells were washed with 1× PBS. Supplemented α-MEM was added to the wells, which were then incubated at 37 °C. ADSCs were collected via trypsinization at the indicated time points: 12, 24, 72, and 96 hours after infection. After spinning for 5 minutes, the ADSCs were resuspended in 200 µl of hypotonic swelling buffer. The virus was released from infected ADSCs by three freeze–thaw cycles. Viral titers were determined as previously described.

Migration. The tropism of ADSCs for glioma cells was determined using an *in vitro* migration assay. ADSCs were labeled with fluorescent dye CM-DiI (Invitrogen, Eugene, OR) as per manufacturer's protocol. U-87 and MRC-5 cells, grown to confluence, were incubated in serum-free media for 48 hours and the resulting conditioned media was aspirated and centrifuged, and the supernatant was placed in the wells of a 24-well plate. ADSCs in serum-free media were placed in the upper well of Millicell hanging cell culture inserts (5 µm; Millipore, Billerica, MA) coated with Matrigel (0.1 mg/ml), which were then placed in each well containing conditioned media. ADSCs were incubated for 48 hours at 37 °C, and the migration ratio was determined by directly counting the number of migrated cells in five high-power fields visualized using fluorescent microscopy.

3D tumor growth assay. This consists of coculturing fluorescent cancer cells with a second noncancer cell population in a Matrigel basement membrane matrix in the absence of serum.[21] The strengths of this assay include (i) experimental tumor cultures (cancer cells plus/minus other cells) are established in complex mixtures of tumor-derived factors; (ii) spatial limitations are greatly reduced when compared to traditional 2D tissue culture systems; (iii) multifaceted 3D cell–cell and cell–extracellular matrix interactions (both physical and soluble) are permitted; (iv) based on fluorescence profiles, different cell types are easily distinguishable. Briefly, U-87 and U-251 GBM cells that stably express the red fluorescent protein, DsRed Express, were cocultured at 10:1 ratio with unlabeled ADSCs, unlabeled WS1, or unlabeled MRC-5. This was embedded in 100 µl of Matrigel (3 mg/ml) and plated in a black 96-well plate. Each condition was plated in triplicate. Red fluorescence was monitored daily for a period of 5 days in a fluorescence plate reader with bottom-read capacity.

3D fluorometric assay. ADSCs were infected with vMyxgfp at an MOI of 10 as previously described. U-87 and U-251 GBM cells that stably express the red fluorescent protein, DsRed Express, were cocultured at 1:1 and 10:1 ratios with unlabeled ADSCs or vMyxgfp-infected ADSCs, and embedded in Matrigel (1 mg/ml). The cultures were terminated after 2- and 4-day time points, and the cells were recovered from the Matrigel matrix with CellSperse (Cultrex; Trevigen, Gaithersburg, MD) treatment. The cell populations were analyzed by flow cytometry.

Animals. Female athymic nude (*nu/nu*) mice, (6–8 weeks old), were purchased from the Animal Production Area of the National Cancer Institute–Frederick Cancer Research and Development Center (Frederick, MD). All animal manipulations were done in accordance with institutional guidelines under approved protocols.

In vivo *studies in an orthotopic glioma model in nude mice.* Animals were randomly split into four groups of four animals. Actively growing U-87 cells were injected at a concentration of 1×10^5 cells in 5 µl PBS alone or co-injected with naive ADSCs, naive MRC-5 cells, or vMyxgfp-infected ADSC, prepared as previously described, at a 1:1 ratio into the right frontal lobe. Mice were anesthetized with a ketamine/xylazine mixture (114/17 mg/kg), and a 0.5 mm burr hole was made 1.5–2 mm right of the midline and 0.5–1 mm posterior to the coronal suture through a scalp incision. Stereotaxic injection used a 10-µl syringe (Hamilton, Reno, NV) with a 30-gauge needle, inserted through the burr hole to a depth of 3 mm, mounted on a Just For Mice stereotaxic apparatus (Harvard Apparatus, Holliston, MA) at a rate of 2 µl/min.

To evaluate the therapeutic effects of ADSCs infected with vMyxgfp (ADSC-vMyxgfp), two groups of four animals received direct intratumoral injection of ADSC-vMyxgfp or naive ADSCs. U-87 cells (1×10^5 in 5 µl PBS) were implanted into the right frontal lobe of athymic nude mice as previously described. After 7 days, when tumors were well established, ADSC-vMyxgfp (2.5×10^5 in 5 µl PBS), or naive ADSCs (2.5×10^5 in 5 µl PBS) were stereotaxically injected directly into the tumor bed in a similar manner as previously described. For assessment of survival, animals were monitored for 120 days at which point the study was arbitrarily terminated.

To evaluate the therapeutic effects of ADSCs infected with vMyxgfp (ADSC-vMyxgfp), two groups of six animals were implanted with U-87 cells (1×10^5 in 5 µl PBS) into the right frontal lobe of athymic nude mice as previously described. Seven days after tumor implantation, intracranial, nonintratumoral injection of 2.5×10^5 ADSCs or 2.5×10^5 vMyxgfp-infected ADSCs into the right hemisphere ~1 mm anterior to the implanted U-87 cells, as previously described above. Fourteen days after tumor implantation and seven days after the first anteriorly placed intracranial, nonintratumoral injection of ADSCs or vMyxgfp-infected ADSCs into the right hemisphere, we administered another intracranial, nonintratumoral injection of 2.5×10^5 ADSCs or 2.5×10^5 vMyxgfp-infected ADSCs into the right hemisphere, ~1 mm posterior to the implanted U-87 cells. We alternated the placement (1 mm anterior or 1 mm posterior to the implanted U-87 cells) of four subsequent intracranial, nonintratumoral injection of ADSCs or vMyxgfp-infected ADSCs into the right hemisphere every 7 days for a total of six intracranial, nonintratumoral therapeutic administrations.

Animals losing ≥20% of their body weight or having trouble ambulating, feeding, or grooming were euthanized by transcardial perfusion.

Histology. Brains were fixed in 4% paraformaldehyde, equilibrated in sucrose, and processed for cryogenic sectioning. Frozen sections were taken at 5 µm and stained for hematoxylin and eosin.

MRI. MRI was performed on a 7T small animal system (Bruker BioSpin, Ettlingen, Germany), equipped with an actively shielded gradient set, with a maximum gradient strength of 400 mT/m. Signal excitation and reception was accomplished with a 25 mm Litz RF coil. Conventional T2-weighted RARE images (echo time = 60 ms, repetition time = 3,000 ms,

© The American Society of Gene & Cell Therapy

slice thickness = 1 mm, matrix = 256 × 256) were acquired in coronal (field of view = 2.5 × 2.5 cm^2) and axial (field of view = 2.2 × 2.2 cm^2) orientations to assess differences in anatomy.

Statistical analysis. GraphPad Prism (version 5; GraphPad Software, San Diego, CA) was used for statistical analyses. Cell viability, cell migration, and cell infection assay results were presented as bar graphs with standard error bars as needed. Cell growth assay results were presented as line graph with standard error bars. Survival curves were generated by Kaplan–Meier method. The log-rank test was used to compare the distributions of survival times, and a P value of <0.05 was considered significant.

SUPPLEMENTARY MATERIAL

Figure S1. Representative fluorescent images illustrating U251 cells co-cultured with ADSCs or vMyxgfp infected ADSCs at a 1:1 ratio.

Figure S2. T2-weighted MR images 38, 51, 66, 78 and 85 days post tumor implantation and after administration of a 6 non-intratumoral injection of myxoma virus infected ADSCs.

Materials and Methods.

Video S1. 3D reconstruction of MRI serial sectioning of a control-treated animal.

Video S2. 3D reconstruction of MRI serial sectioning of a treated animal.

ACKNOWLEDGMENTS

This research was partly funded by the Milheim Foundation, Dana Foundation, and Brain Tumor Center of Excellence from Wake Forest University and the Center for Biomolecular Imaging of Wake Forest University School of Medicine to H.C. D.T.J. was a recipient of the Laura Scales Memorial Fund medical student fellowship, and F.D. was a recipient of the CAPES (Coordenação de Aperfeiçoamento de Pessoal de Nível Superior) scholarship of the Ministério da Educação of the Brazilian government. Special thanks to Todd Atwood for assistance with magnetic resonance imaging. We thank Waldemar Debinski, Wake Forest University for critical review of this manuscript. Viruses and tissue culture reagents and services were provided by the Cell and Virus Vector Core Laboratory of the Comprehensive Cancer Center of Wake Forest University supported, in part, by National Institutes of Health grant CA-12197.

REFERENCES

1. American Cancer Society (2008). *Cancer Facts & Figures* 2008. American Cancer Society: Atlanta, GA.
2. Gurney, JG and Kadan-Lottick, N (2001). Brain and other central nervous system tumors: rates, trends, and epidemiology. *Curr Opin Oncol* **13**: 160–166.
3. Surawicz, TS, Davis, F, Freels, S, Laws, ER Jr and Menck, HR (1998). Brain tumor survival: results from the National Cancer Data Base. *J Neurooncol* **40**: 151–160.
4. Buckner, JC (2003). Factors influencing survival in high-grade gliomas. *Semin Oncol* **30** (6 suppl. 19): 10–14.
5. Stupp, R, Mason, WP, van den Bent, MJ, Weller, M, Fisher, B, Taphoorn, MJ *et al.* (2005). Radiotherapy plus concomitant and adjuvant temozolomide for glioblastoma. *N Engl J Med* **352**: 987–996.
6. Aghi, M and Martuza, RL (2005). Oncolytic viral therapies—the clinical experience. *Oncogene* **24**: 7802–7816.
7. Shah, AC, Benos, D, Gillespie, GY and Markert, JM (2003). Oncolytic viruses: clinical applications as vectors for the treatment of malignant gliomas. *J Neurooncol* **65**: 203–226.
8. Vähä-Koskela, MJ, Heikkilä, JE and Hinkkanen, AE (2007). Oncolytic viruses in cancer therapy. *Cancer Lett* **254**: 178–216.
9. Kerr, P and McFadden, G (2002). Immune responses to myxoma virus. *Viral Immunol* **15**: 229–246.
10. Fenner, F (2000). Adventures with poxviruses of vertebrates. *FEMS Microbiol Rev* **24**: 123–133.
11. Fenner, F and Ross, J (1994). Myxomatosis. In: Thompson, HV and King, CM (eds). *The European Rabbit: The History and Biology of a Successful Colonizer*. Oxford University Press: Oxford. pp. 205–239.
12. Lun, X, Yang, W, Alain, T, Shi, ZQ, Muzik, H, Barrett, JW *et al.* (2005). Myxoma virus is a novel oncolytic virus with significant antitumor activity against experimental human gliomas. *Cancer Res* **65**: 9982–9990.
13. Brower, V (2005). Search and destroy: recent research exploits adult stem cells' attraction to cancer. *J Natl Cancer Inst* **97**: 414–416.
14. Power, AT and Bell, JC (2007). Cell-based delivery of oncolytic viruses: a new strategic alliance for a biological strike against cancer. *Mol Ther* **15**: 660–665.
15. Willmon, C, Harrington, K, Kottke, T, Prestwich, R, Melcher, A and Vile, R (2009). Cell carriers for oncolytic viruses: Fed Ex for cancer therapy. *Mol Ther* **17**: 1667–1676.
16. Aboody, KS, Brown, A, Rainov, NG, Bower, KA, Liu, S, Yang, W *et al.* (2000). Neural stem cells display extensive tropism for pathology in adult brain: evidence from intracranial gliomas. *Proc Natl Acad Sci USA* **97**: 12846–12851.
17. Nakamizo, A, Marini, F, Amano, T, Khan, A, Studeny, M, Gumin, J *et al.* (2005). Human bone marrow-derived mesenchymal stem cells in the treatment of gliomas. *Cancer Res* **65**: 3307–3318.
18. Schäffler, A and Büchler, C (2007). Concise review: adipose tissue-derived stromal cells--basic and clinical implications for novel cell-based therapies. *Stem Cells* **25**: 818–827.
19. Morizono, K, De Ugarte, DA, Zhu, M, Zuk, P, Elbarbary, A, Ashjian, P *et al.* (2003). Multilineage cells from adipose tissue as gene delivery vehicles. *Hum Gene Ther* **14**: 59–66.
20. Zuk, PA, Zhu, M, Mizuno, H, Huang, J, Futrell, JW, Katz, AJ *et al.* (2001). Multilineage cells from human adipose tissue: implications for cell-based therapies. *Tissue Eng* **7**: 211–228.
21. Sasser, AK, Mundy, BL, Smith, KM, Studebaker, AW, Axel, AE, Haidet, AM *et al.* (2007). Human bone marrow stromal cells enhance breast cancer cell growth rates in a cell line-dependent manner when evaluated in 3D tumor environments. *Cancer Lett* **254**: 255–264.
22. Wilcox, ME, Yang, W, Senger, D, Rewcastle, NB, Morris, DG, Brasher, PM *et al.* (2001). Reovirus as an oncolytic agent against experimental human malignant gliomas. *J Natl Cancer Inst* **93**: 903–912.
23. Sypula, J, Wang, F, Ma, Y, Bell, J and McFadden, G (2004). Myxoma virus tropism in human tumor cells. *Gene Ther Mol Biol* **8**: 103–114.
24. Studeny, M, Marini, FC, Dembinski, JL, Zompetta, C, Cabreira-Hansen, M, Bekele, BN *et al.* (2004). Mesenchymal stem cells: potential precursors for tumor stroma and targeted-delivery vehicles for anticancer agents. *J Natl Cancer Inst* **96**: 1593–1603.
25. Wang, G, Barrett, JW, Stanford, M, Werden, SJ, Johnston, JB, Gao, X *et al.* (2006). Infection of human cancer cells with myxoma virus requires Akt activation via interaction with a viral ankyrin-repeat host range factor. *Proc Natl Acad Sci USA* **103**: 4640–4645.
26. Ries, SJ and Brandts, CH (2004). Oncolytic viruses for the treatment of cancer: current strategies and clinical trials. *Drug Discov Today* **9**: 759–768.

Copyright of Molecular Therapy is the property of Nature Publishing Group and its content may not be copied or emailed to multiple sites or posted to a listserv without the copyright holder's express written permission. However, users may print, download, or email articles for individual use.